

ORIGINAL ARTICLE

Open Access



# Theory and Experimental Verification on Cymbal-shaped Slotted Valve Piezoelectric Pump

Jun Huang<sup>1</sup>, Yi-Chao Zhu<sup>1</sup>, Wei-Dong Shi<sup>1</sup> and Jian-Hui Zhang<sup>2\*</sup>

## Abstract

Valve piezoelectric pumps usually have larger flow rate than that of valveless ones. However, the traditional cantilever valve easily induces stress concentration which impacts the reliability of pumps. Therefore, a cymbal-shaped slotted check valve is proposed to be applied in a piezoelectric pump in order to reduce the stress concentration of the valve and thus improve the reliability of the piezoelectric pump. The structure and working principle of the piezoelectric pump are analyzed; the stress analysis of the cymbal-shaped slotted valve diaphragm is conducted. In addition, finite element software is employed to analyze the difference of the Von-Mises stress between the cymbal-shaped slotted diaphragm and the slotted flat diaphragm. The simulation results show that, the Von-Mises stress of cymbal-shaped slotted diaphragm is smaller than that of the slotted flat one. Furthermore, the cymbal-shaped slotted valve piezoelectric pump is also fabricated, and flow rate experiment is performed. The experimental results indicate that the flow rate of piezoelectric pump working in low frequencies ( $0 \text{ Hz} < f < 50 \text{ Hz}$ ) is larger than that working in high frequencies ( $200 \text{ Hz} < f < 2000 \text{ Hz}$ ). When driven at voltage of 160 V and frequency of 5 Hz, the pump reaches its maximum flow rate of 6.6 g/min. The experimental results validate the feasibility of the cymbal-shaped slotted check valve. This research can effectively solve the problem of stress concentration of valve piezoelectric pumps and is helpful for improving the reliability of them.

**Keywords:** Cymbal-shaped slotted, Piezoelectric pump, Valve, Stress

## 1 Introduction

The high requirements of micro-chemical mixing, biological detection and insulin injection raises new actuation requirements in the diversity of actuation functions and types [1–7], and the conventional actuators cannot fulfil these requirements efficiently [8–11]. To meet these requirements, piezoelectric pumps with the merits of rapid response, high energy density, perfect integration, and no electromagnetic interference attracts a large number of researchers [12–24].

Piezoelectric pumps can be sorted by two types, valveless piezoelectric pumps and valve ones, according to whether they have an internal moving part (valve) or not.

Zhang et al. [25] proposed a piezoelectric pump with rotatable unsymmetrical slopes which could be used to piezoelectric liquid mixing and delivery together or separately. Yang et al. [26] designed a bidirectional valveless piezoelectric micropump with double chambers. This pump has better performance at low Reynolds number and can change the flow direction by regulating the voltage.

Compared with valveless piezoelectric pump, valve piezoelectric pump has a larger flow rate and a smaller pulsation, so it has a more extensive application prospect. Hwang et al. [27] designed a reciprocating piezoelectric pump which is used for fuel cells. This pump has the characteristics of compact structure, low energy consumption and even steady output in low driving frequencies. Liu et al. [28] proposed a PZT-based valve piezoelectric pump, and further designed an insulin delivery

\*Correspondence: zhangjh@nuaa.edu.cn

<sup>2</sup> College of Mechanical and Electrical Engineering, Guangzhou University, Guangzhou 510006, China

Full list of author information is available at the end of the article

system in 2014. This piezoelectric pump, with two pump chambers and three passive valves, can achieve a precise supply of drugs by adjusting the voltage and frequency. Wang et al. [29] proposed a piezoelectric pump having a compressible chamber and the valve fixed at its two ends for a fuel cell system in 2014. Due to the fixed passive valve, this pump has a lower leakage and a good output performance working in high frequencies. Ma et al. [30] put forward a separable piezoelectric pump suitable for drug delivery. Due to the separable design between the driving part and the drug delivery unit, this pump can effectively avoid the secondary pollution in drug delivery. Cazorla et al. [31] fabricated a functional micro-pump made of silicon and PZT thin films with standard MEMS technology. This pump characterizes being driven by low voltage.

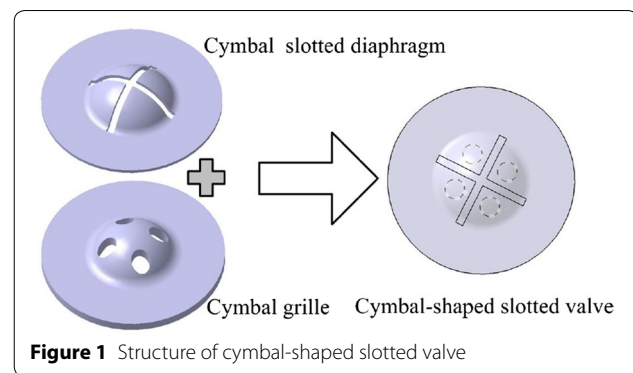
However, the reciprocating motion in a high frequency with the check valve as the pump's core component tends to make the valve generate fatigue damage. Especially when the check valve is working in the fluid, it can generate a large stress which may easily lead to stress concentration, thus aggravating the fatigue damage and causing failure of the check valve. As a result of that, the piezoelectric pump will not work properly.

Ding et al. [32] designed a heart-valve-like check valve by using a structure simulating the working principle of human's heart valve to increase the deformation of the valve and reduce its stress. Based on this structure, a bio-inspired cymbal-shaped slotted valve is proposed in this paper, aiming to largely reduce the stress of the valve under the same loading conditions.

In this research, the structure design of the cymbal-shaped slotted valve is proposed, and working principle of the cymbal-shaped slotted valve piezoelectric pump is analyzed. After theoretically analyzing, the design parameters of the cymbal-shaped slotted valve are achieved. And then, through FEM (Finite Element Method) calculation, the maximum Von-Mises stress on cymbal slotted diaphragm is just 0.036 kPa, which is much smaller than that on the flat one. Finally, the performance of the cymbal-shaped slotted valve piezoelectric pump is tested to verify the validity of the valve.

## 2 Structure and Working Principle

As shown in Figure 1, the cymbal-shaped slotted valve is mainly composed of a cymbal grille and a cymbal slotted diaphragm. When the fluid flows through the valve from grille to diaphragm, the valve is open; when the fluid flows through the valve from diaphragm to grille, the valve is closed. The displacement of the valve changes with the fluid pressure, so it makes the flow rate adjustable. The cymbal-shaped slotted valve piezoelectric pump is mainly composed of a pump cover, a piezoelectric



vibrator, a pump chamber, two cymbal-shaped slotted valves, an inlet tube and an outlet tube, as shown in Figure 2.

When an alternating voltage is applied on the piezoelectric vibrator, the vibrator will do the reciprocating vibration in normal direction due to the inverse piezoelectric effect, causing changes in the volume of the pump chamber. The working principle of cymbal-shaped slotted valve piezoelectric pump is shown in Figure 3. When the piezoelectric vibrator moves upward, the volume of pump chamber increases and the internal pressure reduces. Under the pressure difference between inside and outside of the pump chamber, the fluid in the inlet tube will flow into the pump chamber via grille and diaphragm. In the meantime, the valve at the outlet tube is closed. So the piezoelectric pump at this stage is in the state of suction. Similarly, when the piezoelectric vibrator moves downward, the volume of pump chamber decreases and the internal pressure increases. Under the pressure difference between inside and outside of the pump chamber, the fluid near the outlet tube will flow out of the pump chamber via the valve. In the meantime, the valve at the inlet tube is closed. So the piezoelectric pump at this stage is in the state of discharge.

## 3 Theoretical Analysis

As both the valve's state whether to be open or closed and its reliability are determined by the movement of cymbal slotted diaphragm, it is necessary to make stress analysis of the diaphragm. Mechanics analysis diagram of cymbal-shaped slotted diaphragm is shown in Figure 4 in which a fan zone with angle of  $d\beta$  is arbitrarily selected. The stress deformation of fan-shaped diaphragm is shown in (a) and equivalent simplified diagram is shown in (b) of Figure 4.

Where the meanings of each parameter in Figure 4 are expressed as follows:  $\xi$  is radial displacement of the cymbal slotted diaphragm;  $f$  is bending displacement;  $\delta$  is axial displacement;  $\Delta$  is tensile deformation;  $h_0$  is the height of the diaphragm;  $t_m$  is the thickness of the

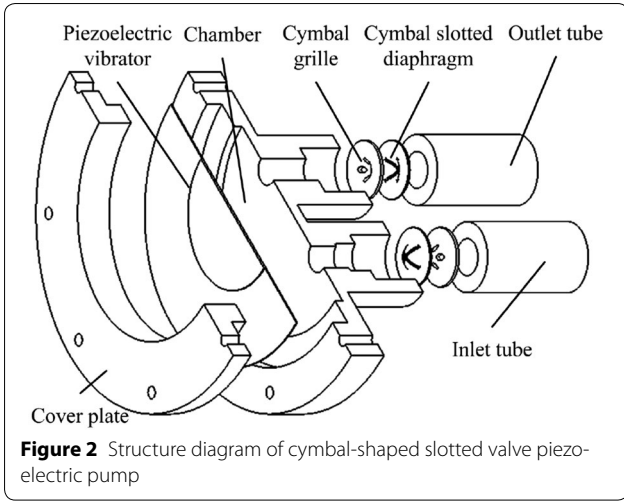


**Figure 2** Structure diagram of cymbal-shaped slotted valve piezo-electric pump

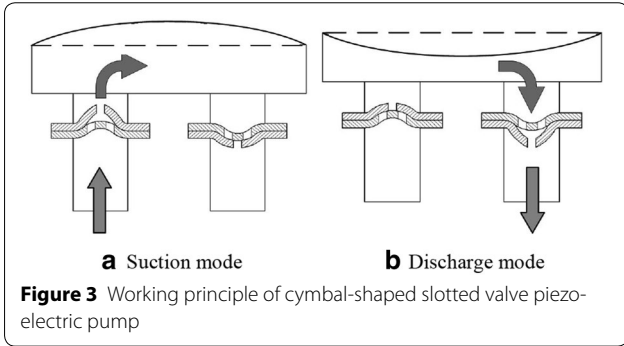


**Figure 3** Working principle of cymbal-shaped slotted valve piezo-electric pump

diaphragm;  $E$  is elastic modulus;  $\theta$  is the cone angle;  $r_1$ ,  $r_2$  and  $r_0$  are respectively the top, bottom and overall radius of the diaphragm;  $b$  is the arc length at arbitrary position  $x$ ,

$$b = \frac{xb_1}{r_1} = \varphi(x). \tag{1}$$

The inertia moment  $I_x$  at  $x$  is

$$I_x = \frac{bt_m^3}{12} = \frac{t_m^3}{12}\varphi(x), \tag{2}$$

where  $OA = r_2$ ,  $AB = r_1$ ,  $F = qx$ . To obtain the deformation of the cantilever at position  $A$ , a virtual force  $F_e$  is loaded at arbitrary position on part  $OB$ , provided  $AC = a$ , then solve it by using the principle of virtual work:

$$M_{AB} = qx \cdot \frac{1}{2}x, \tag{3}$$

$$M_{BC} = qr_1 \left(x - \frac{1}{2}r_1\right) + q(x - r_1)\frac{1}{2}(x - r_1), \tag{4}$$

$$M_{CO} = qr_1 \left(x - \frac{1}{2}r_1\right) + q\frac{1}{2}(x - r_1)^2 + F_e(x - a) \tag{5}$$

The total energy is

$$U = \int \frac{M_x^2}{2EI_x} dx = \frac{1}{2E} \left( \int_0^{r_1} \frac{M_{AB}^2}{I_x} dx + \int_{r_1}^a \frac{M_{BC}^2}{I_x} dx + \int_a^{r_2} \frac{M_{CO}^2}{I_x} dx \right), \tag{6}$$

$$f_c = \frac{\partial U}{\partial F_e} \Big|_{F_e=0} = \frac{1}{E} \int_a^{r_2} \frac{\left[qr_1 \left(x - \frac{1}{2}r_1\right) + \frac{1}{2}q(x - r_1)^2\right](x - a)}{\frac{t_m^3}{12}\varphi(x)} dx = \frac{6q}{Et_m^3\varphi(x)} \left(\frac{1}{3}r_2^3 - \frac{1}{2}ar_2^2 + \frac{1}{6}a^3\right). \tag{7}$$

When  $a = r_1$ ,

$$f_c = \frac{6q}{Et_m^3\varphi(x)} \left(\frac{1}{3}r_2^3 - \frac{1}{2}r_1r_2^2 + \frac{1}{6}r_1^3\right). \tag{8}$$

When the virtual force is loaded at point  $C$  on part  $AB$ ,

$$M_{BC} = qx\frac{1}{2}x + F_e(x - a), \tag{9}$$

$$M_{BO} = qr_1 \left(x - \frac{1}{2}r_1\right) + F_e(x - a) + q\frac{1}{2}(x - r_1)^2. \tag{10}$$

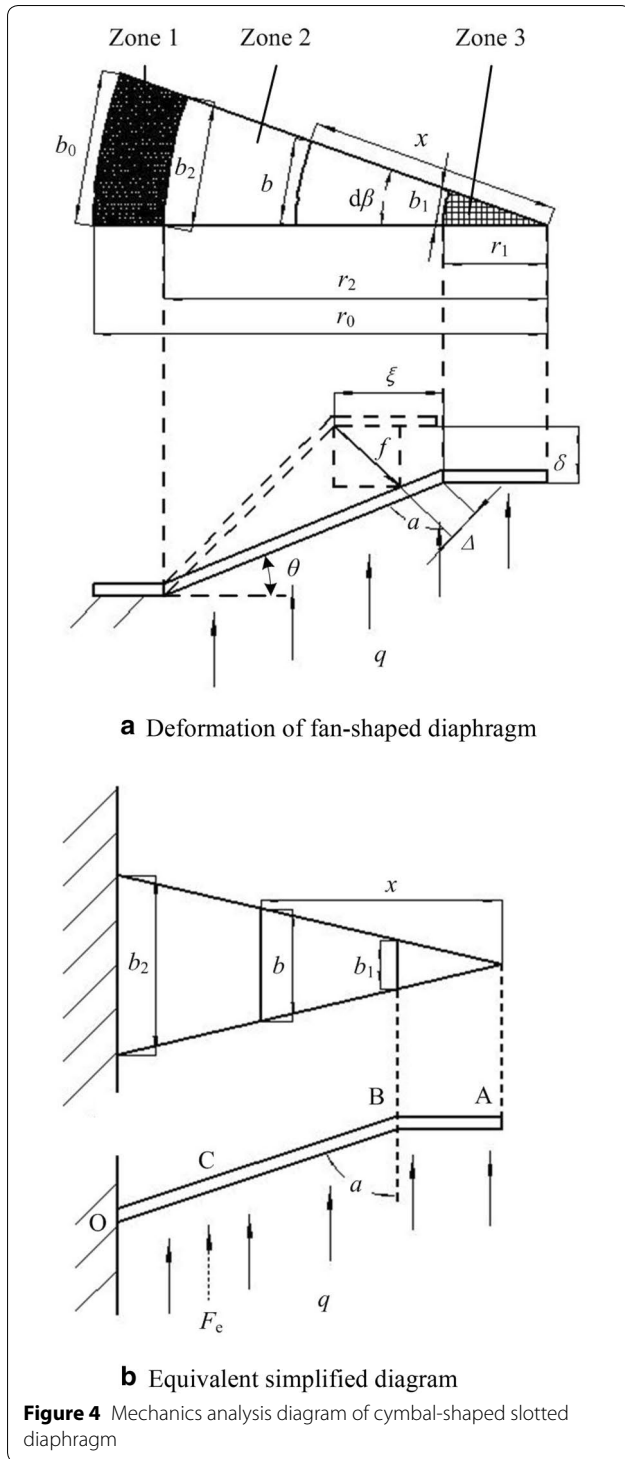
The total energy is

$$U' = \int \frac{M_x^2}{2EI_x} dx = \frac{1}{2E} \left( \int_a^{r_1} \frac{F_e(x - a)qx^2}{I_x} dx \right) + U, \tag{11}$$

$$f'_c = \frac{\partial U'}{\partial F_e} \Big|_{F_e=0} = \frac{1}{2E} \int_a^{r_1} \frac{qx}{\frac{t_m^3}{12}\varphi(x)} dx + f_c = \frac{6q}{Et_m^3\varphi(x)} \left(\frac{1}{3}r_1^3 - \frac{1}{2}ar_1^2 + \frac{1}{6}a^3 + \frac{1}{3}r_2^3 - \frac{1}{2}ar_2^2 + \frac{1}{6}a^3\right). \tag{12}$$

When  $a = 0$ ,

$$f'_c = \frac{6q}{Et_m^3\varphi(x)} \left(\frac{1}{3}r_1^3 + \frac{1}{3}r_2^3\right) = \frac{2q}{Et_m^3\varphi(x)} (r_1^3 + r_2^3). \tag{13}$$



The tensile deformation of the valve is

$$\varepsilon = \frac{d\Delta}{dx} = \frac{F}{EA} = \frac{qr_2 \cos \theta}{Et_m \varphi(x)}, \quad (14)$$

where  $A$  is the cross-sectional area of the valve, and  $\Delta$  is a tensile variable of the valve. According to the boundary conditions, tensile deformation of the valve can be obtained as follows:

$$\Delta = \int_{r_1}^{r_2} \frac{qr_2 \cos \theta}{Et_m \varphi(x)} dx = \frac{qr_2 \cos \theta}{Et_m \varphi(x)} \ln \frac{r_2}{r_1}. \quad (15)$$

The radial displacement is

$$\begin{aligned} \xi &= f'_c \sin \theta + \Delta \cos \theta \\ &= \frac{2q}{Et_m^3 \varphi(x)} (r_1^3 + r_2^3) \sin \theta + \frac{qr_2 \cos^2 \theta}{Et_m \varphi(x)} \ln \frac{r_2}{r_1}. \end{aligned} \quad (16)$$

The axial displacement is

$$\begin{aligned} \delta &= f'_c \cos \theta - \Delta \sin \theta \\ &= \frac{2q}{Et_m^3 \varphi(x)} (r_1^3 + r_2^3) \cos \theta - \frac{qr_2 \sin \theta \cos \theta}{Et_m \varphi(x)} \ln \frac{r_2}{r_1}, \end{aligned} \quad (17)$$

$$\frac{r_2 - r_1}{h_0} = \tan \theta, \quad (18)$$

where  $r_2$  and  $r_1$  can be regarded as constant values. The range of the angle  $\theta$  is  $0^\circ \leq \theta < 90^\circ$ . The smaller  $\theta$  is, the larger  $\xi$  will be, and  $\delta$  decreases at first then increases. That is, under the same external conditions, the lower the cymbal slotted diaphragm is, the larger its radial displacement will be, and its axial displacement decreases at first then increases. It can be seen that, when  $\theta$  is  $0^\circ$ , the cymbal slotted diaphragm becomes a flat slotted diaphragm,  $\delta$  reaches its maximum. This shows that, under the same external conditions, the axial displacement of the flat slotted diaphragm is greater than that of the cymbal-shaped ones. And when  $\theta$  tends to  $90^\circ$ , the diaphragm will only move radially.

#### 4 Finite Element Analysis

Three-dimensional modeling via finite element method is conducted for the cymbal-shaped slotted diaphragm and the slotted flat diaphragm to compare their Von-Mises stresses under the same loading conditions. Structure parameters of cymbal-shaped slotted diaphragm and the slotted flat diaphragm are shown in Table 1. Their models

**Table 1** Parameters of slotted diaphragm mm

Parameter	Diaphragm thickness $d_0$	Projected diameter $D$	Width of the slot $\delta$	Length of the slot $l$
Value	0.2	9.6	0.5	4

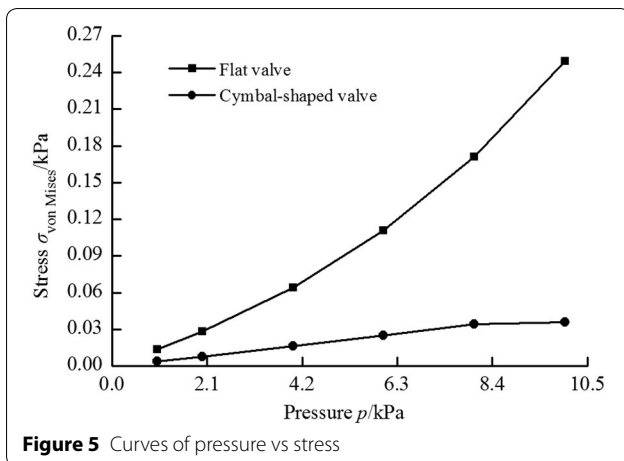


Figure 5 Curves of pressure vs stress

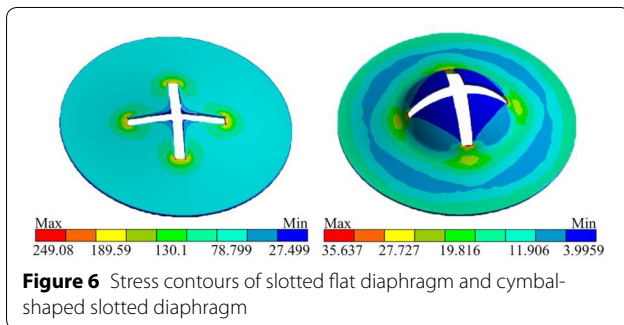


Figure 6 Stress contours of slotted flat diaphragm and cymbal-shaped slotted diaphragm

Table 2 Geometrical parameters of vibrator mm

Parameter name	Diameter of PZT $d_1$	Thickness of PZT $h_1$	Diameter of copper $d_2$	Thickness of copper $h_2$
Value	25	0.2	50	0.2

are imported into Ansys Workbench, then meshed and set with the boundary conditions, and applied the same alternating load to calculate the their Von-Mises stresses so as to analyze the feasibility of the valve. In this research, the models of the slotted diaphragms were divided into more than 3000 tetrahedron elements. The edges of the diaphragms have ‘zero displacement’ boundary conditions, so the diaphragms could be considered to be fixed supported.

The curves of pressure vs stress are shown in Figure 5. It shows that when the frequency of alternating pressure load applied on them is 10 Hz, with the increase of the load amplitude, the stress of both diaphragms will gradually increase; under the same pressure load, the cymbal-shaped slotted diaphragm is obviously smaller than the slotted flat diaphragm in stress, and with increase of the

Table 3 Geometrical parameters of pump chamber, diaphragm and grille mm

Parameter name	Diaphragm thickness $h_3$	Grille thickness $h_4$	Chamber diameter $d_3$	Chamber depth $h_5$
Value	0.2	0.5	40	1.5

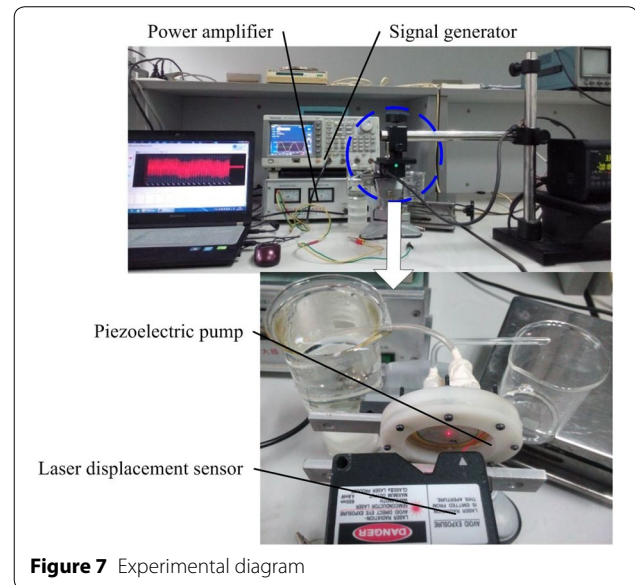


Figure 7 Experimental diagram

pressure load, the difference between their stress will also increase.

When the load amplitude is 10 kPa, the Von-Mises stress contours of slotted flat diaphragm and cymbal slotted diaphragm are shown in In Figure 6. It shows that their maximum stress are both located in the root of the slot. Under this load, the slotted flat diaphragm has its maximum Von-Mises stress of 0.249 kPa, and the cymbal slotted diaphragm 0.036 kPa.

### 5 Experimental Verification and Discussions

A prototype of the cymbal-shaped slotted valve piezoelectric pump has been manufactured. Its pump cover, pump chamber, inlet tube and outlet tube, and the cymbal grille are shaped by 3D printing photosensitive resin material. The cymbal slotted diaphragm is made of beryllium bronze with high elasticity. The geometrical parameters of piezoelectric vibrator are shown in Table 2, and the geometrical parameters of pump chamber, diaphragm and grille are shown in Table 3.

The photos about a physical piezoelectric pump and its performance test are shown in Figure 7 (Additional file 1: Experimental video). To eliminate the generation of bubbles in the test, deionized water was used as the

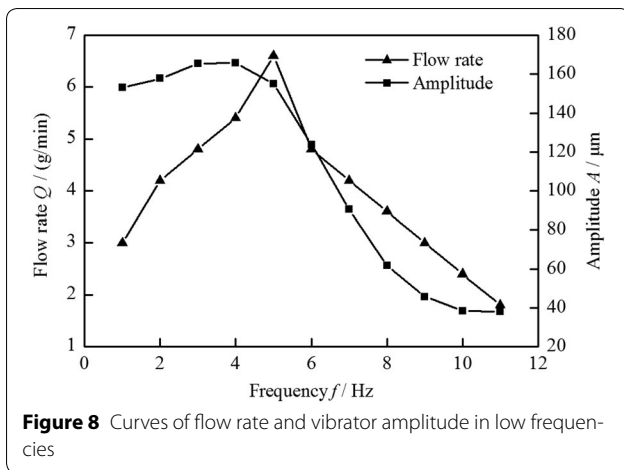


**Figure 8** Curves of flow rate and vibrator amplitude in low frequencies

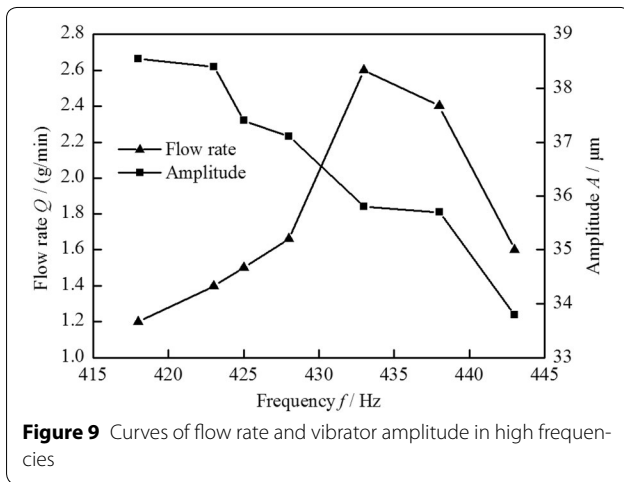


**Figure 9** Curves of flow rate and vibrator amplitude in high frequencies

working fluid. Driving voltage in the test was a peak value of 160 V, and the pump’s mass output per unit time was measured by varying the driving frequency of the piezoelectric vibrator, so that piezoelectric pump’s curve of flow rate vs frequency can be obtained. In the meantime, laser displacement sensor (LK-G30, Keyence Inc., Japan) was used to measure the displacement of the center of the piezoelectric vibrator to obtain the relationship between the amplitude of the piezoelectric vibrator and driving frequency. Flow rate and the amplitude of vibrator in the test are shown in Figure 8 and Figure 9.

As shown in Figure 8, when the vibrator is working in low frequencies, with the increase of driving frequency, both the piezoelectric pump’s flow rate and vibrator amplitude present to increase at first then decrease. When the driving frequency is 4 Hz, the piezoelectric vibrator has its maximum amplitude of 165.8  $\mu\text{m}$ ; when the driving frequency is 5 Hz, the piezoelectric pump has its maximum flow rate of 6.6 g/min. The reason for the

driving frequency at maximum vibrator amplitude being different from that at maximum flow rate is that the flow rate of the piezoelectric pump depends on the volume change in pump chamber per unit time, that is, the flow rate is associated with vibrator amplitude and the driving frequency, therefore, the vibrator amplitude can’t completely determine the flow rate.

As shown in Figure 9, when the vibrator is working in high frequencies, with the increase of driving frequency, the piezoelectric pump’s flow rate presents to increase at first then decrease, while the vibrator amplitude is gradually reducing. When the driving frequency is 433 Hz, the piezoelectric pump has its maximum flow rate of 2.6 g/min. In addition to the factor of the volume change of pump chamber, the reason for the driving frequency at maximum vibrator amplitude being different from that at maximum flow rate also lies in the pump’s valve hysteresis characteristics [21].

## 6 Conclusions

- (1) To solve the disadvantages of valve piezoelectric pump, such as valve’s large stress, easy to get damaged, low reliability of the pump, a cymbal-shaped slotted check valve is proposed to be applied in a piezoelectric pump. Based on the theoretical analysis of cymbal slotted diaphragm, it can be seen that the displacement of the diaphragm (flow rate of the piezoelectric pump) has a correlation with the height of cymbal slotted diaphragm.
- (2) The finite element software is employed to calculate the stresses of the cymbal slotted diaphragm and the slotted flat diaphragm. When the frequency of alternating pressure load applied on them is 10 Hz and the magnitude of the load is 10 kPa, cymbal slotted diaphragm has its maximum Von-Mises stress which is 0.036 kPa, and the slotted flat diaphragm is 0.249 kPa. That is, the cymbal slotted diaphragm is smaller than the slotted flat diaphragm in stress, so the cymbal slotted diaphragm has a high reliability.
- (3) A prototype of the cymbal-shaped slotted valve piezoelectric pump has been manufactured, and the pump performance was tested. The results show that: both the pump’s maximum flow rate and the maximum vibrator amplitude turn out to be at a low frequency; when the driving voltage is 160 V and the driving frequency is 4 Hz, the pump reaches its maximum flow rate which is 6.6 g/min; when the driving frequency is 5 Hz, the piezoelectric vibrator has its maximum amplitude which is 165.8  $\mu\text{m}$ . This test validates the feasibility of the cymbal-shaped slotted check valve piezoelectric pump.

### Authors' contributions

J-HZ proposed the cymbal-shaped slotted check valve and carried out the studies in the reviews of the principles of the cymbal-shaped slotted valve piezoelectric pump. JH fabricated the cymbal shaped slotted valve piezoelectric pump and performed flow rate experiment. He wrote the draft. Y-CZ conducted the stress analysis of the cymbal-shaped slotted valve diaphragm and carried out the finite element simulation. W-DS provided the fabrication method of the cymbal-shaped slotted valve. All authors read and approved the final manuscript.

### Author details

<sup>1</sup> National Research Center of Pumps, Jiangsu University, Zhenjiang 212013, China. <sup>2</sup> College of Mechanical and Electrical Engineering, Guangzhou University, Guangzhou 510006, China.

### Authors' Information

Jun Huang, born in 1981, is currently an assistant professor at *National Research Center of Pumps, Jiangsu University, China*. He received his PhD degree from *Nanjing University of Aeronautics and Astronautics, China*, in 2014. His current research focuses on piezoelectric actuators and sensors.

Yi-Chao Zhu, born in 1992, is currently a master candidate at *Research Center of Fluid Machinery Engineering and Technology, Jiangsu University, China*.

Wei-Dong Shi, born in 1964, is currently a professor and a PhD candidate supervisor at *Jiangsu University, China*. His research area is fluid machinery seal technology and optimization design of pump devices. E-mail: wdshi@ujs.edu.cn

Jian-Hui Zhang, born in 1963, is currently a professor and a PhD candidate supervisor at *Guangzhou University, China*. His research area is mechanical design and its theory, piezoelectric driving.

### Acknowledgements

Supported by National Natural Science Foundation of China (Grant No. 51605200), Jiangsu Provincial Natural Science Foundation of China (Grant No. BK20150518), Jiangsu Provincial Postdoctoral Science Foundation of China (Grant No. 1501108B), and Senior Talent Start-up Foundation of Jiangsu University (Grant No. 14JDG145).

### Competing interests

The authors declare that they have no competing interests.

### Ethics approval and consent to participate

Not applicable.

### Publisher's Note

Springer Nature remains neutral with regard to jurisdictional claims in published maps and institutional affiliations.

### Additional File

**Additional file 1** Experimental video of piezoelectric pump.

Received: 6 July 2016 Accepted: 15 January 2018

Published online: 28 February 2018

### References

1. J H Park, M Y Seo, Y B Ham, et al. A study on high-output piezoelectric micropumps for application in DMFC. *Journal of Electroceramics*, 2012, 30(1–2): 102–107.
2. J W Kan, M Xuan, Z G Yang, et al. Analysis and test of piezoelectric micropump for drug delivery. *Journal of Biomedical Engineering*, 2005, 22(4): 809–813. (in Chinese)
3. G J Liu, Z Q Fan, J S Dong, et al. Piezoelectric micro pump for insulin injection. *Journal of Jilin University (Engineering and Technology Edition)*, 2007, 37(2): 372–376. (in Chinese)
4. M L Cantwell, F Amirouche, J Citerin. Low-cost high performance disposable micropump for fluidic delivery applications. *Sensors & Actuators A Physical*, 2011, 168(1): 187–194.
5. T Zhang, Q M Wang. Valveless piezoelectric micropump for fuel delivery in direct methanol fuel cell (DMFC) devices. *Journal of Power Sources*, 2005, 140(1): 72–80.
6. Y Xu, Z T Hu, M Guo. Design of micropump for parallel multi-parameter detection of microbial metabolic components based on electrochemical platform. *Chinese Journal of Sensors and Actuators*, 2015, 28(1): 1–8. (in Chinese)
7. C S Zhang, D Xing, Y Y Li. Micropumps, microvalves, and micromixers within PCR microfluidic chips: Advances and trends. *Biotechnology Advances*, 2007, 25(5): 483–514.
8. Y Wang, W Q Huang. A piezoelectric motor with two projections using two orthogonal flexural vibration modes. *Sensors & Actuators A Physical*, 2016, 250: 170–176.
9. L Wang, C Y Shu, J M Jin, et al. A novel traveling wave piezoelectric actuated tracked mobile robot utilizing friction effect. *Smart Material Structures*, 2017, 26(3): 035003.
10. H Lee, Y Choi. A new actuator system using dual-motors and a planetary gear. *IEEE/ASME Transactions on Mechatronics*. 2011, 17(1): 192–197.
11. A D Poole, J D Booker, Wishart C L, et al. Performance of a prototype travelling-wave actuator made from a dielectric elastomer. *IEEE/ASME Transactions on Mechatronics*, 2011, 17(3): 525–533.
12. J H Zhang, Y Wang, J Fu, et al. Advances in Technologies of Piezoelectric Pumping with Valves. *Transactions of Nanjing University of Aeronautics & Astronautics*, 2016, 33(3): 260–273.
13. Q X Xia, J H Zhang, H Lei, et al. Analysis on flow field of the valveless piezoelectric pump with two inlets and one outlet and a rotating unsymmetrical slopes element. *Chinese Journal of Mechanical Engineering*, 2012, 25(3): 474–483.
14. Z H Zhang, J W Kan, G M Cheng, et al. A piezoelectric micropump with an integrated sensor based on space-division multiplexing. *Sens. Actuators A: Phys.*, 2013, 203(6): 29–36.
15. Y Luo, X Yin, X Wang, et al. Vibration performances of polymeric micropump actuated by PbZrTiO<sub>3</sub> bimorph. *Micro & Nano Letters*, 2013, 8(8): 559–562.
16. L Liang, X Ma, T M Zhang. Structure design and simulation of circular ring piezoelectric peristaltic pump. *Transactions of the Chinese Society of Agricultural Engineering*, 2012, 28(11): 40–44. (in Chinese)
17. T Q Truong, N T Nguyen. A polymeric piezoelectric micropump based on lamination technology. *Journal of Micromechanics & Microengineering*, 2004, 14(4): 632–638.
18. J Huang, J H Zhang, W D Shi, et al. 3D FEM analyses on flow field characteristics of the valveless piezoelectric pump. *Chinese Journal of Mechanical Engineering*, 2016, 29(4): 825–831.
19. J H Zhang, Y Wang, J Huang. Advances in Valveless Piezoelectric Pump with Cone-shaped Tubes. *Chinese Journal of Mechanical Engineering*, 2017, 30(4): 766–781.
20. H H Kim, J H Oh, J N Lim, et al. Design of valveless type piezoelectric pump for micro-fluid devices. *Transactions on Electrical & Electronic Materials*, 2009, 1(1): 353–356.
21. J H Zhang, D K Wang, S Y Wang, et al. Research on piezoelectric pump-lagging of valve. *Chinese Journal of Mechanical Engineering*, 2003, 39(5): 107–110. (in Chinese)
22. J Huang, J H Zhang, S Y Wang, et al. Analysis of the flow rate characteristics of valveless piezoelectric pump with fractal-like Y-shape branching tubes. *Chinese Journal of Mechanical Engineering*, 2014, 27(3): 628–634.
23. E Sayar, B Farouk. Multifield analysis of a piezoelectric valveless micropump: effects of actuation frequency and electric potential. *Smart Materials & Structures*, 2012, 21(7): 416–422.
24. H K Ma, H C Su, J Y Wu. Study of an innovative one-sided actuating piezoelectric valveless micropump with a secondary chamber. *Sensors & Actuators A Physical*, 2011, 171(2): 297–305.

25. J H Zhang, Q X Xia, Y Huang, et al. Theory and experimental verification of piezoelectric pump with rotatable unsymmetrical slopes. *Science China Technological Science*, 2011, 54(11): 3070–3077.
26. S Yang, X H He, S Q Yuan, et al. A bidirectional valveless piezoelectric micropump with double chambers based on Coanda effect. *Journal of the Brazilian Society of Mechanical Sciences and Engineering*, 2016, 38(2): 345–353.
27. J Y Hwang, K Y Shin, S H Lee, et al. Periodic fuel supply to a micro-DMFC using a piezoelectric linear actuator. *J. Micromech. Microeng.*, 2010, 20(8): 85023–85029.
28. G J Liu, Z G Yang, J F Liu, et al. A low cost, high performance insulin delivery system based on PZT actuation. *Microsystem Technologies*, 2014, 20(12): 2287–2294.
29. X Y Wang, Y T Ma, G Y Yan, et al. High flow-rate piezoelectric micropump with two fixed ends polydimethylsiloxane valves and compressible spaces. *Sensors & Actuators A Physical*, 2014, 218(10): 94–104.
30. H K Ma, W F Luo, J Y Lin. Development of a piezoelectric micropump with novel separable design for medical applications[J]. *Sensors & Actuators A Physical*, 2015, 236: 57–66.
31. P H Cazorla, O Fuchs, M Cochet, et al. A low voltage silicon micro-pump based on piezoelectric thin films. *Sensors & Actuators A Physical*, 2016, 250: 35–39.
32. C C Zhang, T Guo, G F Ding. Passive micro-valve based on SU-8. *Opt. Precision Eng.*, 2013, 21(4): 1011–1016. (in Chinese)

**Submit your manuscript to a SpringerOpen<sup>®</sup> journal and benefit from:**

- ▶ Convenient online submission
- ▶ Rigorous peer review
- ▶ Open access: articles freely available online
- ▶ High visibility within the field
- ▶ Retaining the copyright to your article

---

Submit your next manuscript at ▶ [springeropen.com](http://springeropen.com)

---